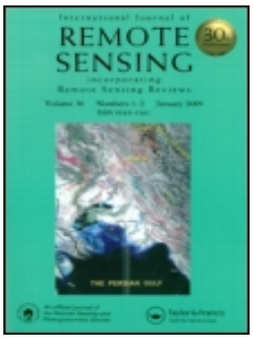

International Journal of Remote Sensing

ISSN: 0143-1161 (Print) 1366-5901 (Online) Journal homepage: www.tandfonline.com/journals/tres20

The Satellite Application Facility for Land Surface Analysis

Isabel F. Trigo, Carlos C. Dacamara, Pedro Viterbo, Jean-Louis Roujean, Folke Olesen, Carla Barroso, Fernando Camacho-de-Coca, Dominique Carrer, Sandra C. Freitas, Javier García-Haro, Bernhard Geiger, Françoise Gellens-Meulenberghs, Nicolas Ghilain, Joaquín Meliá, Luis Pessanha, Niilo Siljamo & Alirio Arboleda

To cite this article: Isabel F. Trigo, Carlos C. Dacamara, Pedro Viterbo, Jean-Louis Roujean, Folke Olesen, Carla Barroso, Fernando Camacho-de-Coca, Dominique Carrer, Sandra C. Freitas, Javier García-Haro, Bernhard Geiger, Françoise Gellens-Meulenberghs, Nicolas Ghilain, Joaquín Meliá, Luis Pessanha, Niilo Siljamo & Alirio Arboleda (2011) The Satellite Application Facility for Land Surface Analysis, International Journal of Remote Sensing, 32:10, 2725-2744, DOI: 10.1080/01431161003743199

To link to this article: https://doi.org/10.1080/01431161003743199

Published online: 24 May 2011.

International Journal of Remote Sensing
Vol. 32, No. 10, 20 May 2011, 2725–2744

Taylor & Francis
Taylor & Francis Group

The Satellite Application Facility for Land Surface Analysis

ISABEL F. TRIGO*†‡, CARLOS C. DACAMARA‡, PEDRO VITERBO†‡, JEAN-LOUIS ROUJEAN§, FOLKE OLESEN¶, CARLA BARROSO†, FERNANDO CAMACHO-DE-COCA|, DOMINIQUE CARRER§, SANDRA C. FREITAS†, JAVIER GARCÍA-HARO|, BERNHARD GEIGER§, FRANÇOISE GELLENS-MEULENBERGHS¤, NICOLAS GHILAIN¤, JOAQUÍN MELIÁ|, LUIS PESSANHA†, NIILO SILJAMO¥ and ALIRIO ARBOLEDA¤

†Instituto de Meteorologia, Lisbon, Portugal
‡Instituto Dom Luiz, Lisbon, Portugal
§CNRM/GAME, Météo-France/CNRS, Toulouse, France
¶Forschungszentrum Karlsruhe, Institut für Meteorologie und Klimaforschung, Karlsruhe, Germany
|Departament de Termodinàmica, Universitat de Valencia, Valencia, Spain
¤Department of Research and Development, Royal Meteorological Institute, Brussels, Belgium
¥Finnish Meteorological Institute, Earth Observation, Helsinki, Finland

(*Received 10 December 2008; in final form 19 February 2010*)

Information on land surface properties finds applications in a range of areas related to weather forecasting, environmental research, hazard management and climate monitoring. Remotely sensed observations yield the only means of supplying land surface information with adequate time sampling and a wide spatial coverage. The aim of the Satellite Application Facility for Land Surface Analysis (Land-SAF) is to take full advantage of remotely sensed data to support land, land–atmosphere and biosphere applications, with emphasis on the development and implementation of algorithms that allow operational use of data from European Organization for the Exploitation of Meteorological Satellites (EUMETSAT) sensors. This article provides an overview of the Land-SAF, with brief descriptions of algorithms and validation results. The set of parameters currently estimated and disseminated by the Land-SAF consists of three main groups: (*i*) the surface radiation budget, including albedo, land surface temperature, and downward short- and longwave fluxes; (*ii*) the surface water budget (snow cover and evapotranspiration); and (*iii*) vegetation and wild-fire parameters.

1. Introduction

The Satellite Application Facility for Land Surface Analysis (Land-SAF) is part of the SAF network, a set of specialized development and processing centres serving the European Organization for the Exploitation of Meteorological Satellites (EUMETSAT) Application Ground Segment (Schmetz *et al*. 2002). The SAF network complements the product-oriented activities at the EUMETSAT Central

*Corresponding author. Email: Isabel.Trigo@meteo.pt

International Journal of Remote Sensing
ISSN 0143-1161 print/ISSN 1366-5901 online
http://www.tandf.co.uk/journals
DOI: 10.1080/01431161003743199

Facility in Darmstadt. The main purpose of the Land-SAF is to take full advantage of remotely sensed data, particularly those available from EUMETSAT sensors, to measure land surface variables, which will find applications primarily in meteorology.

The Land-SAF makes use of two main satellite systems: the geostationary series, Meteosat Second Generation (MSG), and the EUMETSAT Polar System (EPS). With respect to the previous generation of European geostationary satellites, the spin-stabilized MSG has an imaging-repeat cycle of 15 min (against 30 min on the previous system), which provides more timely information. The EPS is Europe's first polar orbiting operational meteorological satellite and the European contribution to a joint polar system with the US. EUMETSAT will have the operational responsibility for the 'morning orbit' with Meteorological-Operational (MetOp) satellites, the first of which was launched successfully on 19 October 2006.

The Spinning Enhanced Visible and Infrared Imager (SEVIRI) radiometer, onboard MSG, has unique spectral characteristics and accuracy, with a 3 km resolution (sampling distance) at nadir (1 km for the high-resolution visible channel), and 12 spectral channels (table 1; Schmetz *et al*. 2002). Its combination with the Advanced Very High Resolution Radiometer (AVHRR) onboard MetOp permits global coverage of the land surface, with AVHRR complementing SEVIRI at high latitudes.

The Land-SAF (figure 1) started its 5-year development phase in September 1999, and its initial operations in January 2005. During the current phase of the project, from March 2007 to February 2012, the Land-SAF consortium is pursuing the consolidation of its operational and user support activities. Emphasis is on the validation and upgrading of algorithms based on the changing needs of the users and full exploitation of the capabilities of EUMETSAT sensors. The Land-SAF has been especially designed to serve the needs of the meteorological community, particularly Numerical Weather Prediction (NWP). The products retrieved from Meteosat and EPS satellites can be grouped into (*i*) Surface Radiation Budget parameters, which include downward long- (DSLF) and shortwave (DSSF) surface fluxes, albedo (AL), land surface temperature (LST), and emissivity (EM); and (*ii*) Biogeophysical parameters, such as snow cover (SC), soil moisture and evapotranspiration (ET), and vegetation products (table 2). The growing number of users in agricultural and

Table 1. Characteristics of the Spinning Enhanced Visible and Infrared Imager (SEVIRI) onboard Meteosat Second Generation (www.eumetsat.int).

Channel	Central wavelength (μm)	Dynamic range	Radiometric noise
VIS0.6	0.635	533 W m^{-2} sr^{-1} μm^{-1}	S/N 10 at 1% albedo
VIS0.8	0.81	357 W m^{-2} sr^{-1} μm^{-1}	S/N 7 at 1% albedo
NIR1.6	1.64	75 W m^{-2} sr^{-1} μm^{-1}	S/N 3 at 1% albedo
IR3.9	3.92	335 K	0.35 K at 300 K
WV6.2	6.25	300 K	0.75 K at 250 K
WV7.3	7.35	300 K	0.75 K at 250 K
IR8.7	8.70	300 K	0.28 K at 300 K
IR9.7	9.66	310 K	1.50 K at 255 K
IR10.8	10.80	335 K	0.25 K at 300 K
IR12.0	12.00	335 K	0.37 K at 300 K
IR13.4	13.40	300 K	1.80 K at 270 K
HRV	Broadband (about 0.4–1.1)	460 W m^{-2} sr^{-1} μm^{-1}	S/N 1.2 at 0.3% albedo

S/N, Signal-to-noise ratio.

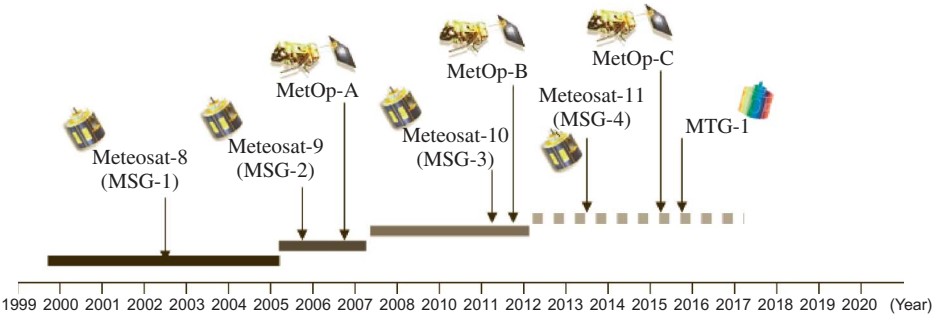

Figure 1. Project phases: (*i*) 5-year development period (September 1999 to December 2004); (*ii*) initial operations phase (January 2005 to February 2007); and (*iii*) the continuous development and operations phase, which began in March 2007. The schedule for EUMETSAT satellite launches is also indicated.

forestry applications, land use, and the broader topics of climate, environment monitoring and atmospheric chemistry, have supported the extension of biogeophysical parameters to wild-fire-related products. The Land-SAF generates land surface variables on a pixel-by-pixel basis, which are provided to users in the satellite nominal resolution, for most of the products. An indication of the expected accuracy of each retrieved value is also given, either in the form of quality flags or as an estimated error range (i.e. estimates of product inaccuracy taking into account known algorithm uncertainties and propagation of input errors).

User requirements evolve with the availability of improved or new data sources, and the rise of potential applications for new products. Programmes promoted by the World Meteorological Organization (WMO) or by the European Commission (EC) and European Space Agency (ESA), such as the Global Monitoring for Environment and Security (GMES), have established guidelines for the monitoring of climate and environment, stressing the need for global, long-term, high quality and reliable products. The life cycle of EUMETSAT satellites, and the participation of Land-SAF consortium members in the *geoland* project (a prototype for the land component of GMES), put the Land-SAF in a privileged position as a product/service provider for those programmes. Finally, the proactive relationship with the user community is expected to be reinforced through cooperation with users regarding validation activities, and through promotion of workshops to discuss the adequacy of the Land-SAF list of products, and their respective characteristics (workshop proceedings, with examples of product application, are available at http://landsaf.meteo.pt/workshops.jsp).

2. Surface radiation budget

2.1 *Products and algorithms*

Surface radiation budget-related parameters have been estimated from SEVIRI/MSG, archived and disseminated on a regular basis since March 2005. Estimations using AVHRR/MetOp and merging of polar orbiting and geostationary satellite data are now foreseen for 2009. Polar orbiters will improve spatial coverage at high latitudes, as well as the angular sampling for a better estimation of surface albedo. Land surface albedo (AL) is the fraction of incoming solar energy reflected at the

Table 2. Current Land-SAF products (operational or under development). SEVIRI channels used per product; the horizontal resolution and spatial coverage, generation frequency, and target accuracy are also indicated. Temporal resolution specifies the time interval for composite products. The use of AVHRR/MetOp data (and ASCAT/MetOp in the case of SC and ET) for product enhancement (increase spatial coverage; improve accuracy) is currently being considered.

	Product	SEVIRI channels	Horizontal resolution and coverage	Temporal resolution	Generation frequency	Target accuracy
Surface radiation budget	Albedo (AL)	VIS 0.6, 0.8 IR 1.6	MSG disc‡	5-day and 30-day	Daily and 10-day	For AL > 0.15: 10%; < 0.15: 0.01
	Land surface temperature (LST)	IR 10.8, 12.0	MSG disc‡/ global*	Instantaneous	15min and 12-hourly*	2 K
	Downwelling surface shortwave flux	VIS 0.6, 0.8 IR1.6	MSG disc‡/ global*	Instantaneous and daily	30 min and daily	above 200 W m^{-2}: 10%; below 200 W m^{-2}: 20 W m^{-2}
	Downwelling surface longwave flux	VIS 0.6, 0.8 IR 1.6, 3.9, 8.7, 10.8, 12.0, 13.4, WV 7.3†	MSG disc‡/ global*	Instantaneous and daily	30 min and daily	10%
Biogeophysical parameters I	Snow cover (SC)	VIS 0.6, IR3.9, 10.8, 12.0	MSG disc‡/ global	Daily	Daily	False alarm: 15%; hit rate: 80%
	Evapotranspiration (ET)	†	MSG disc‡	Daily/30 min	Daily/30 min	> 0.4 mm h^{-1}: 25%; < 0.4 mm h^{-1}: 0.1 mm h^{-1}
Biogeophysical parameters II	Fraction vegetation cover (FVC)	VIS 0.6, 0.8 IR1.6	MSG disc‡/ global*	5-day and 30-day	Daily and 10-day	15%
	Lead area index (LAI)	VIS 0.6, 0.8 IR 1.6	MSG disc‡/ global*	5-day and 30-day	Daily and 10-day	1
	Fraction of absorbed photosynthetically active radiation (FAPAR)	VIS 0.6, 0.8	MSG disc‡/ global*	5-day and 30-day	Daily and 10-day	15%
	Risk of fire mapping	†	Europe	Daily	Daily	–
	Fire detection and monitoring	VIS 0.6, 0.8 IR 3.9, 10.8, 12.0	MSG disc‡	Daily	15 min	False alarm: 6%; hit rate: 50%, using MODIS as reference
	Fire radiative power (FRP)	VIS 0.6, IR 1.6, 3.9, 10.8, 12.0	MSG disc‡	Daily/15 min	Hourly/15 min	70% of retrieved FRP within 50% of 'true' values as defined by MODIS

*Global and 12-hourly products refer to retrievals from AVHRR/EPS.
†Indirectly, through other Land-SAF components (AL, DSSF, DSLF, FVC, LAI, clouds, etc.).
‡MSG spatial resolution ranges from 3 km around nadir to pixel sampling distances of the order of 5, 6 and 9 km for areas over Europe at around 40, 50 and 60° N, respectively.

surface. It indirectly quantifies the fraction of the energy that is absorbed and transformed into surface sensible and latent heat fluxes. Owing to strong feedback effects, the knowledge of albedo is important for determining weather conditions in the atmospheric boundary layer (Dickinson 1983). The Land-SAF AL product (Geiger *et al.* 2008a) is based on the three shortwave channels at 0.6, 0.8 and 1.6 μm. In the first step of the AL processing chain, cloud-free reflectance observations of each time-slot are corrected for atmospheric effects using the simplified radiative transfer code SMAC (Rahman and Dedieu 1994). A linear kernel-driven bidirectional reflectance distribution function (BRDF) model (Roujean *et al.* 1992) is then inverted against daily time series of top-of-canopy reflectance values. The integration of the BRDF model provides spectral AL values that are then converted into broadband estimates corresponding to visible (e.g. figure 2(*a*)), near-infrared, and total (e.g. figure 2(*b*)) shortwave ranges. These are available as directional-hemispherical ('black-sky') and bi-hemispherical ('white-sky') quantities (Geiger *et al.* 2008a). Two temporal AL products are considered: one with an effective temporal scale of 5 days, updated on a daily basis, and a 30-day composite, updated every 10 days. The temporal resolution associated with the former reduces the sensitivity to uncorrected atmospheric effects (e.g. residual cloudiness), while still being able to detect short-term variations of the surface properties, such as recent snowfall or burnt areas. Median values of error estimates for the 5-day AL are of the order of 0.005, while the 90th centile is around 0.010. Nevertheless, the reliability of AL retrievals (both 5-day and 30-day products) may be degraded (*i*) over regions with persistent cloud cover, as is often the case in tropical areas during the rainy season; (*ii*) over areas with very high aerosol loads, since the current version of the AL algorithm relies on aerosol climatological data for the atmospheric correction; and (*iii*) over pixels with recent snowfall or snow melt. Users may easily identify such cases, associated with larger error ranges and degraded quality flags.

The monthly composite AL samples (sub-)seasonal time-scales. The Land-SAF Team is currently working on an improved version of the 30-day AL composite, which makes use of observations provided by SEVIRI/MSG (for multiple illumination angles) and AVHRR/MetOp (for different viewing geometries). The

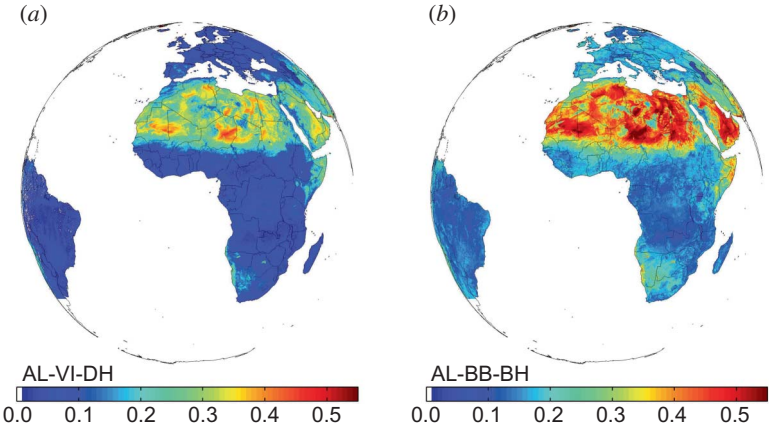

Figure 2. Albedo estimated for 10 July 2006: (*a*) visible (range 0.4–0.7 μm) black sky; and (*b*) total shortwave (range 0.4–4 μm) white sky albedo.

combination of data sets from geostationary and polar systems is indeed challenging because it requires some harmonized effort relative to the data preprocessing (cloud and aerosol removal). The expected improvements in BRDF quality with a better angular resolution will be operated typically at 3 km spatial resolution. This value corresponds to a compromise as it represents the SEVIRI subsatellite footprint and an average resolution for AVHRR between nadir (1 km) and off-nadir (6 km).

Land surface temperature (LST), or directional radiometric temperature of the surface, provides the best approximation to the thermodynamic temperature based on a radiance measurements (Norman and Becker 1995). It should be kept in mind, however, that directional effects are important for heterogeneous and non-isothermal surfaces, such as a satellite pixels over land (Barroso *et al*. 2005, Trigo *et al*. 2008a). There, thermodynamic temperature would be better represented by the hemispherical radiometric temperature (Norman and Becker 1995). Currently, the Land-SAF LST (figure 3(*a*)) is obtained by correcting top-of-atmosphere (TOA) radiances for the atmospheric attenuation along the path and the reflection of downward radiance. The LST algorithm is based on a generalized split window, following the formulation first proposed by Wan and Dozier (1996) to derive LST from the AVHRR and Moderate Resolution Imaging Spectroradiometer (MODIS), adapted to SEVIRI data (Trigo *et al*. 2008a). Surface temperature is estimated as a linear function of clear-sky, TOA brightness temperatures for the split-window channels 10.8 μm and 12.0 μm, where regression coefficients depend explicitly on land surface emissivity for each channel, and implicitly on atmospheric water vapour content and satellite viewing angle. Channel and broadband emissivity is estimated as a weighted average of that of bare ground and vegetation elements within each pixel (Peres and DaCamara 2005, Trigo *et al*. 2008b), using the fraction of vegetation cover (FVC), another Land-SAF product described below. The uncertainty of LST retrievals (figure 3(*b*)) takes into account the inaccuracy inherent in the generalized split-windows method and the propagation of errors in the input variables (Freitas *et al*. 2010). The field presented in figure 3(*b*) depicts well the regions with lower LST accuracy (error ranges above 3 K), namely: (*i*) arid areas where the uncertainty in surface emissivity is generally high, and

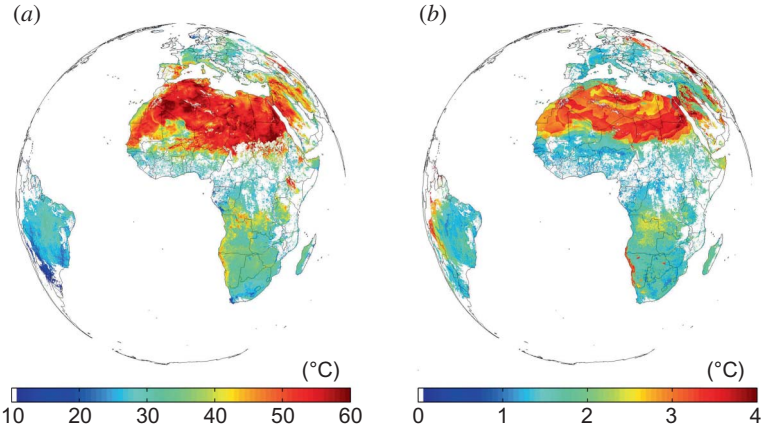

Figure 3. (*a*) Land surface temperatures (LSTs) estimated for 10 July 2006, 12 UTC and (*b*) the uncertainty of the LST retrievals. White areas over continents correspond to cloudy pixels, where LST was not retrieved.

where the extreme high brightness temperatures tend to further enhance LST error ranges; and (*ii*) regions near the border of the MSG disc, where large optical paths associated with high viewing angles lead to large LST uncertainties, particularly in the presence of moist atmospheres.

Information on cloud cover is obtained using the Nowcasting and Very Short Range Forecasting Satellite Application Facility (SAFNWC) software (http://www.nwcsaf.org/HD/Main.jsp). Dynamic information on the atmospheric pressure and total column water vapour comes from the European Centre for Medium-range Weather Forecasts (ECMWF) NWP model. Cloud data (identification and cloud type classification) are used in the processing of all Land-SAF products, either to flag non-processed pixels (e.g. BRDF, LST) or to be used for the estimation of atmospheric absorption/emission within the visible (VIS)/infrared(IR) domain needed for the estimation of the respective downward fluxes at the surface.

The downwelling surface short- and longwave radiation fluxes (DSSF and DSLF) refer to the radiative energy flux in the wavelength intervals 0.3–4.0 μm and 4–100 μm, respectively. Both DSSF and DSLF products are calculated for every second slot of MSG input data at intervals of 30 min. The estimates are derived for the instantaneous acquisition time of each image line. Satellite-derived estimates of radiation fluxes are valuable tools to validate results from assimilation systems and climate models (Allan *et al*. 2004, Harries *et al*. 2005, Bony *et al*. 2006) or off-line forcing of land surface models (Dirmeyer *et al*. 2006).

The shortwave component, DSSF (figure 4(*a*)), essentially depends on the solar zenith angle, cloud cover and, to a lesser extent, atmospheric absorption and surface albedo. The methodology for the retrieval of DSSF implemented in the Land-SAF system (Geiger *et al*. 2008b) relies on the approach developed within the framework of the Ocean and Sea Ice (OSI) SAF (Brisson *et al*. 1999). The distinguishing features of the Land-SAF product are the spatial and temporal resolution, the source of ancillary input data, and the use of three shortwave SEVIRI channels (0.6, 0.8 and 1.6 μm). DSSF is strongly anti-correlated with observed TOA reflectances; bright clouds (i.e. high TOA reflectances) correspond to low solar radiation reaching the surface. Estimated TOA albedo serves as the most important input information for a simple

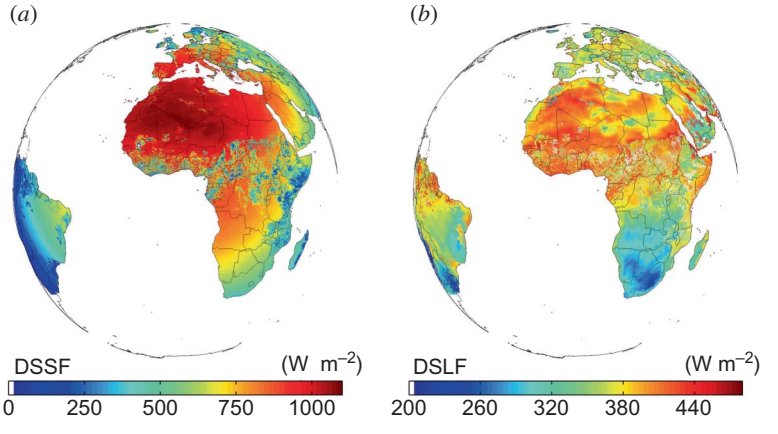

Figure 4. (*a*) Shortwave and (*b*) longwave downwelling fluxes at the surface (W m^{-2}), estimated for 10 July 2006, 12 UTC.

physical parameterization of the radiation transfer in the cloud–atmosphere–surface system. In clear-sky conditions DSSF is estimated directly by a parameterization for the effective transmittance of the atmosphere as a function of the concentration of atmospheric constituents (Frouin *et al*. 1989). For cloudy situations, DSSF estimates rely on a simplified physical description of the radiation transfer in the cloud–atmosphere–surface system (Gautier *et al*. 1980, Brisson *et al*. 1999). Important elements of this scheme are cloud transmittance, cloud albedo, and atmospheric transmittance between the surface and clouds. Estimates for the cloud properties are derived from TOA albedo (Geiger *et al*. 2008b), determined from the satellite measurements by applying a broadband conversion relationship (Clerbaux *et al*. 2005) and an angular dependence model (Manalo-Smith *et al*. 1998).

The estimation of DSLF (figure 4(*b*)) combines remotely sensed information on clouds and atmospheric fields (temperature and humidity) provided by NWP models. In the Land-SAF approach, DSLF makes use of bulk parameterization schemes merging formulations derived for clear-sky conditions (e.g. Prata 1996), with schemes developed for cloudy skies (e.g. Josey *et al*. 2003). DSLF retrievals benefit from the signature of clouds and different cloud types on IR and VIS channels, complemented with information on atmosphere water content and near-surface air temperature available from NWP fields, also used to estimate atmospheric transmittance in the DSSF algorithm. It is worth noting that NWP fields, obtained from ECMWF 12- to 24-h forecasts, include information from atmospheric sounders and other observations, and thus correspond to the best knowledge of atmospheric profiles for each time slot.

2.2 *Validation of radiative parameters*

The validation strategy for Land-SAF products focuses on three main aspects: (*i*) comparison with similar parameters retrieved from different sensors; (*ii*) comparison with *in-situ* measurements; and (*iii*) sensitivity studies and assessment of the impact of input errors on the quality of the Land-SAF products. The latter are the basis for the estimation of the product error range for each retrieved value, which is disseminated to users (see, for example, figure 3(*b*)). Validation of surface radiative fluxes makes use of the Baseline Surface Radiation Network (BSRN) (http://www.bsrn.awi.de), a project of the World Climate Research Programme (WCRP) and the Global Energy and Water Experiment (GEWEX) aimed at detecting important changes in the Earth's radiation field (Ohmura *et al*. 1998). BSRN radiation measurements include surface downwelling short- and longwave fluxes and more rarely upwelling fluxes. As a result of a strict quality control, BSRN data have been widely used to validate radiation schemes in climate modelling and to check the calibration of satellite-derived radiometric products. To overcome the scarcity of LST ground measurements within the area covered by Meteosat, the Land-SAF Team carried out exploratory studies to find suitable LST validation sites and one LST ground-truth station has already been set up in Évora (Southern Portugal), in operation since August 2005 (Kabsch *et al*. 2008). Recently, two other sites have been set up in Africa, in Namibia and Senegal, respectively.

As an example, figure 5 presents results from different methodologies involved in the validation of Land-SAF radiation products, including comparison with similar parameters retrieved from MODIS (LST and albedo), and with *in situ* measurements (DSSF and DSLF). Validation exercises not only provide information on product

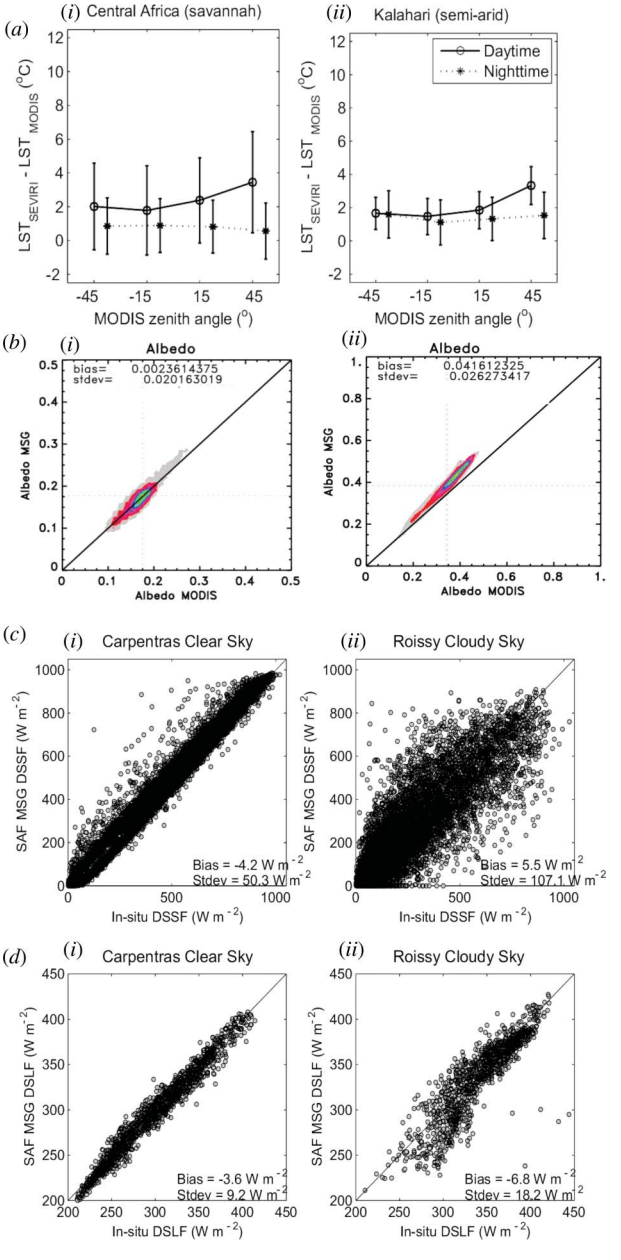

Figure 5. Examples of validation exercises carried out for radiation parameters, including comparison with products from other satellites and *in situ* observations. (*a*) Average and standard deviation (°C) differences between SEVIRI and MODIS LST products for two 10° × 10° boxes in Africa, centred at (*i*) 10° S, 20° E (Central Africa and (*ii*) 25° S, 20° E (Kalahari). The statistics are obtained for the period 25–31 July 2005, for MODIS daytime and night-time passages (see legend), and for the classes of MODIS satellite zenith angle specified on the *x*-axis. (*b*) Land-SAF broadband bidirectional albedo (*y*-axis) retrieved (*i*) over Europe (10–25 June 2006) and (*ii*) over Northern Africa (12–27 July 2006), plotted against the equivalent MODIS parameter (*x*-axis); average (bias) and standard deviation (Stdev) of differences are also indicated. (*c*) Scatterplot of Land-SAF DSSF versus *in situ* measurements for (*i*) clear-sky cases observed in Carpentras, France and (*ii*) cloudy conditions observed in Roissy, France. The data were collected between 2006 and 2007. (*d*) Scatterplot of Land-SAF DSLF versus *in situ* measurements for same cases as in (*c*).

accuracy but also reveal product characteristics and problematic/optimal retrieval conditions. The comparison between Land-SAF (SEVIRI) and MODIS LST (figure 5(*a*)) shows a clear dependence of discrepancies with viewing angles, for daytime cases. As discussed in detail in Trigo *et al.* (2008a), these results indicate clearly the directional character of remotely sensed LST, and also suggest that comparison of night-time estimates is more suitable for the detection of biases associated with the algorithm or input data. Overall, SEVIRI LST is higher than MODIS LST, with night-time systematic differences ranging between 0.5°C and 1.0°C. Similarly, Land-SAF SEVIRI AL is routinely compared with MODIS AL (figure 5(*b*)). The results reveal very good matching between the two parameters. Over northern Africa, characterized by very bright surfaces, the Land-SAF product generates higher broadband albedo values (figure 5(*b*)(*ii*)). Such overestimation with respect to MODIS albedo is primarily linked to differences in angular integration of surface reflectances, due either to the use of different BRDF models or diverse angular samplings (more details in Geiger *et al.* 2008a).

Although not shown, the validation of LST and AL products includes evaluation against *in situ* measurements. Figures 5(*c*) and 5(*d*) show, also as an example, scatterplots of Land-SAF downward fluxes for DSSF and DSLF, respectively, versus ground observations for two stations in France. The results are presented separately for clear and cloudy-sky conditions, revealing higher discrepancies for the latter, as expected. In general, the radiative fluxes are within the target accuracy (table 2) for most retrieved values. Conditions likely to produce lower quality estimates (e.g. partially clouded pixels, high angle observations) are flagged within the retrieved products. In addition, DSSF (DSLF) may be overestimated (underestimated) under very high aerosol loads, as shown by Slingo *et al.* (2006).

Product validation is essential for assessing whether user requirements (table 2) are met. The example presented in figure 5 aims to illustrate the ongoing validation of surface radiation parameters, using both *in situ* observations and data from other satellites. Further detailed results on product performance may be found in the Land-SAF validation reports updated regularly (http://landsaf.meteo.pt; see also Geiger *et al.* 2008a,b, Kabsch *et al.* 2008, Trigo *et al.* 2008a,b).

3. Biogeophysical parameters

3.1 *Water budget*

In addition to the surface radiation budget, the Land-SAF has been tasked to provide a series of biogeophysical products, essential for modelling and understanding land surface processes. SC and ET constitute the first set, related to the surface water budget.

SC relies on different signatures of snow, ice and clouds on the reflectance of shortwave IR channels onboard SEVIRI/MSG and AVHRR/MetOp to provide daily fields discriminating snow-free, snow-covered and partially snow-covered pixels over the whole European area. As the separation between cloud and surface ice/snow is also crucial for cloud detection, the SC algorithm is based on a thresholding procedure to distinguish surfaces covered with snow or ice from clouds and snow-free pixels. The resulting SC (http://landsaf.meteo.pt) product has been generated on an operational basis and archived since March 2005. An additional set of quality/processing flags for each pixel is provided to users, giving information on the uncertainty of the classification (further details may be found in the respective *Product User Manual*, Land-SAF 2006). Table 3 presents a summary of the Land-SAF SC scores

Table 3. Land-SAF snow cover product verified against NOAA/NESDIS (Europe; July 2007–February 2009).

Proportion correct	0.977
Bias	0.863
Probability of detection	0.747
False alarm rate	0.135

using the National Oceanic and Atmospheric Administration (NOAA)/National Environmental Satellite, Data and Information Service (NESDIS) product as reference. The statistics corresponding to SC retrievals over the European region, between July 2007 and February 2009, show good agreement between the two products. Detection of snow with VIS and IR is generally less reliable for terrains with steep slopes, or over areas with dense forests with snow under the canopy. These cases are flagged in the Land-SAF SC product.

Although SC estimations based on IR and VIS channels provide maps with high spatial resolution, they may be hampered by persistent cloudiness; in this respect, the high temporal sampling of geostationary satellites provides a clear advantage towards polar orbiters. The information from both platforms will be used to produce daily SC maps, which will be particularly useful over the mid- to high latitudes. In regions such as Central and Eastern Europe or Scandinavia, Meteosat viewing geometry makes the detection of snow more difficult because of the high satellite zenith angles, and radiances correspond to coarser spatial resolution pixels (with distances between pixels reaching 6–12 km). There the better spatial resolution provided by MetOp, along with observations closer to nadir, will complement the higher observation frequency of Meteosat. Microwave data are not limited to clear-sky observations, they are also sensitive to snow water equivalent (e.g. Kongoli *et al.* 2004, Drusch *et al.* 2004). However, they have coarser resolution (typically 25–50 km, instead of 1–5 km) and may present problems in the detection of thin or wet snow (Kongoli *et al.* 2004). The accuracy of snow products derived from VIS/IR and from microwave varies considerably with surface and terrain types and atmospheric conditions. Merging the two different sources of data will provide the best means to improve accuracy, extend product availability, and provide information on snow metamorphism (snow ageing, melting, ice). The Land-SAF Team expects to minimize known sources of errors by introducing, for example, topographic and land cover corrections (e.g. forests).

One of the aims of the Land-SAF is the estimation of parameters necessary for a complete description of the energy budget over land surfaces, making use of EUMETSAT. Within this framework, ET, which combines soil and intercepted water evaporation with plant transpiration, is essential to the estimation of surface latent heat flux.

The approach currently followed to derive ET makes use of a soil–vegetation–atmosphere transfer (SVAT) model – a simplified version of the ECMWF TESSEL SVAT scheme – forced by Land-SAF radiation products (DSSF, DSLF and AL) and ECMWF meteorology to estimate ET. Soil moisture will be estimated through Advanced Scatterometer (ASCAT)/MetOp data, through either direct assimilation of TOA radiances or soil moisture retrievals (provided by EUMETSAT). ET depends on many local factors and variables (e.g. vegetation type and state, soil moisture, near surface wind), making its validation particularly difficult. Figure 6 shows a scatterplot of Land-SAF ET estimates against observations taken in Cabauw (The Netherlands),

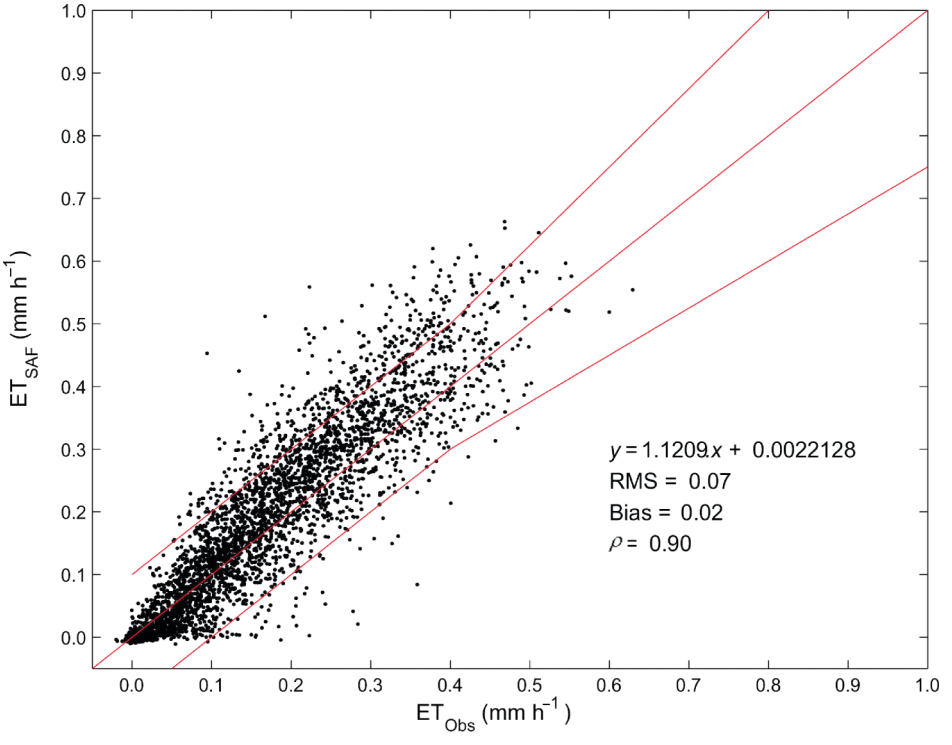

Figure 6. Comparison of 30-min Land-SAF evapotranspiration (ET_SAF) estimates (mm h^{-1}) with *in-situ* measurements (ET_Obs) taken in Cabauw (The Netherlands) over the period ranging from 1 March to 31 December 2007.

characterized by grassland (Beljaars and Bosveld 1997). The comparison with observations does not present evident systematic biases. In general, the validation results reveal good agreement between estimations and observations obtained for stations in areas dominated by grasslands (figure 6) and mixed forests (not shown; Land-SAF 2008). So far, validation of ET has been mostly performed for Europe. Flux measurements over Africa and South America are scarcer but a full assessment of Land-SAF ET estimations over those regions is ongoing.

At a later stage, the Land-SAF Team expects to test alternative approaches to the estimation of daily ET by exploiting the spectral and temporal resolution of SEVIRI. Among others, Caparrini *et al.* (2004) showed that sequential LST data contain useful information on the partitioning of available surface energy into latent and sensible surface heat fluxes. Thus, high frequency (e.g. 15-min) fields of LST may be assimilated into an SVAT model, which can also use other surface radiation parameters as forcing.

3.2 *Vegetation and wild fires*

The second set of biogeophysical parameters comprises vegetation and wild fire indices. Fraction of Vegetation Cover (FVC), Leaf Area Index (LAI), and Fraction of Absorbed Photosynthetically Active Radiation (FAPAR) are currently retrieved from SEVIRI; retrievals based on AVHRR and on merged AVHRR and SEVIRI

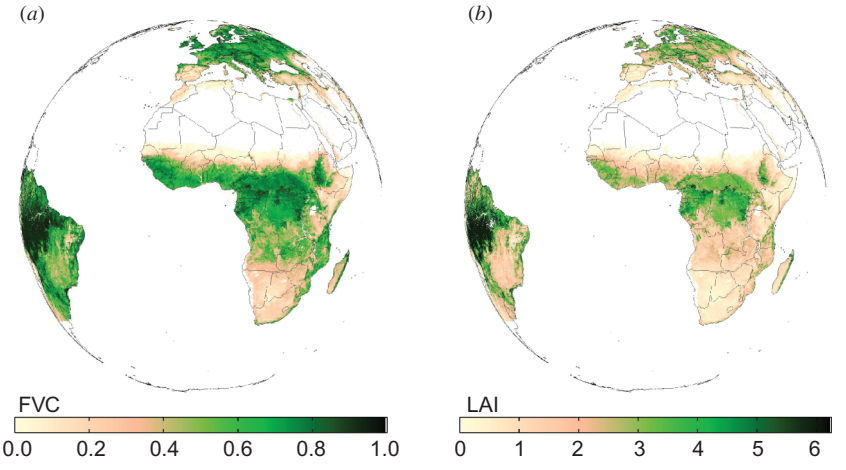

Figure 7. (*a*) Fraction of Vegetation Cover (FVC) and (*b*) Leaf Area Index (LAI), corresponding to a 5-day composite, estimated on 10 July 2006.

data will become available later. FVC (figure 7(*a*)) characterizes the fraction of vegetation on a flat background; LAI (figure 7(*b*)) is a dimensionless variable (m^2 m^{-2}) defined as one half of the total leaf area per unit ground area, and accounts for the surface of leaves contained in a vertical column normalized by its cross-sectional area; and FAPAR (not shown) represents the fraction of solar energy absorbed by vegetation for photosynthesis. FVC, LAI and FAPAR are relevant parameters for a wide range of land–biosphere applications, from agriculture and forestry to environmental management and land use. FVC determines the partition between soil and vegetation contributions, also used for emissivity estimations. For fully and healthy developed canopies, LAI indicates the amount of green vegetation that absorbs or scatters solar radiation, and is an important parameter in NWP, climate and SVAT models. Finally, FAPAR is an indicator of the health and thereby productivity of vegetation. FAPAR is generally well correlated with LAI, particularly for healthy, fully developed, vegetation canopies.

The algorithms of the vegetation products rely on the use of BRDF parameters (Roujean and Lacaze 2002), which contain specific spectral directional signatures of vegetation reflectances. The normalization of SEVIRI images to a common geometry minimizes surface anisotropy effects, which constitute one of the main drawbacks of using geostationary satellites for vegetation monitoring. While FAPAR is based on simulations of surface reflectances in optimal angular geometries (Roujean and Bréon 1995), FVC is estimated through the application of a spectral mixture analysis methodology, developed taking into account the spectral variability of vegetation in different ecosystems (e.g. Bateson *et al.* 2000, García-Haro *et al.* 2005), to VIS and near-IR reflectance values. The algorithm relies on a statistical approach, in which soil and vegetation components are represented by a multimodal probability density function. Finally, LAI is estimated from FVC following the methodology developed by Roujean and Lacaze (2002), which proved to be more effective than traditional techniques based on spectral vegetation indices.

The high rate of acquisition provided by the SEVIRI instrument guarantees the availability of spatially consistent cloud-free data for adequately monitoring both the

seasonality of vegetation and the long-term trends in the state of vegetation. The spatial and temporal variation of the SEVIRI vegetation products in Southern Africa was validated using data collected by Privette *et al.* (2002) and Huemmrich *et al.* (2005) along the International Geosphere Biosphere Programme (IGBP) Kalahari Transect. A representative example of this analysis is presented in figure 8. LAI retrieved from SEVIRI/MSG captures the phenology in this area, from peak-biomass in March–April (towards the end of the wet season), to senescence, peak dry season and minimum foliar biomass in early September, and rapid green-up into the next season. Large product errors are generally found at high latitudes, particularly over Europe during winter, since the inputs are derived under suboptimal conditions. Product limitations at high latitudes are anticipated to be considerably reduced by combining SEVIRI and AVHRR data. Moreover, the quality of FVC, LAI and FAPAR also tends to be degraded for areas with persistent cloud, high aerosol loads, or large viewing angles, as in the case of the AL product. Such degradation is reflected in the product error range, and in extreme cases (e.g. very large input uncertainties, or traces of snow) the estimated values are masked out. In the case of FAPAR, values with estimated uncertainty higher than 0.25 are set to 'not processed' in the final product files. The information on retrieval conditions or on the reasons for ignoring the retrieval is detailed in the product quality flags. Maps of estimated error ranges for FVC, LAI and FAPAR (not shown) generally exhibit high values over high latitudes, particularly during winter, and along the most active areas of the Inter-Tropical Convergence Zone (ITCZ). Uncertainty estimates, based on the propagation of input errors and on the theoretical uncertainty of the algorithm, typically range between 0.04 and 0.15 for FVC, between 0.03 and 0.10 for LAI, and between 0.05 and 0.15 for FAPAR.

Fire-related processes have long been identified as applications with great potential to be derived from SEVIRI/MSG and AVHRR/MetOp (Pereira and Govaerts 2001, Boschetti *et al.* 2003). These applications include the monitoring of vegetation susceptibility to fire, which is linked to water stress and surface temperature. The merging

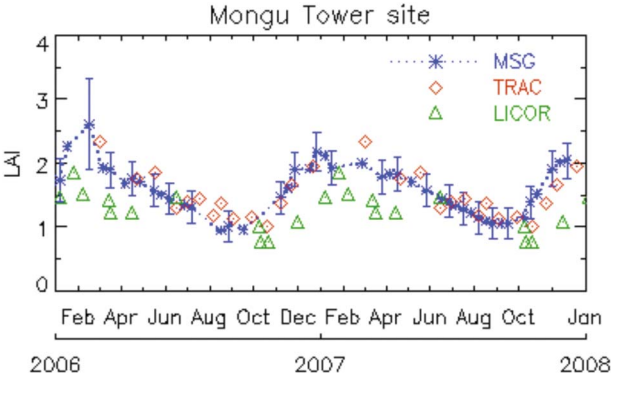

Figure 8. Comparison of Land-SAF LAI product (stars; labelled MSG) retrieved from SEVIRI over a 2-year period (2006–2007) with (non-concomitant) field measurements over the Mongu site in western Zambia (15.438 S, 23.253 E). The land-cover type at the site is a Miombo woodland on Kalahari sand (woody savannah). The single time-profile combines all measurements taken with two different instruments and periods: (*i*) TRAC instrument (Natural Resources Canada, Canada Centre for Remote Sensing, Ontario, Canada) over the year 2000 (diamonds) and (*ii*) LAI-2000 LICOR instrument (Li-COR Biosciences, Lincoln, NE, USA) over the period 2000–2002 (triangles).

of such data with meteorological parameters provides indicators of fire risk, fire detection, monitoring and fire scar identification. Following demands from environment monitoring and risk management (e.g. GMES requirements), the Land-SAF is currently exploring (*i*) the capability of SEVIRI/MSG to detect and monitor active fires, particularly over Africa, leading to the operational generation, archiving and dissemination of the Fire Detection and Monitoring (FD&M) product; and (*ii*) signals of vegetation water stress on SEVIRI channels (0.8, 1.6 and 3.9 μm), to follow its variability in space and time, and to produce a meaningful danger of fire rating, or Risk of Fire Mapping (RFM), for (Southern) Europe. The latter is still under development; an operational version is currently foreseen for the end of 2010.

Biomass burning is a significant global source of aerosols, greenhouse gases (e.g. carbon dioxide and methane) as well as of nitric and carbon monoxides, methyl bromide and hydrocarbons that lead to acid rain and the photochemical production of tropospheric ozone and destruction of stratospheric ozone, which impact global climate (e.g. Crutzen and Andreae 1990). Other impacts of biomass burning relate to the biogeochemical cycling of nitrogen and carbon compounds, the hydrological cycle, the reflectivity and emissivity of the land, the stability of ecosystems and ecosystem biodiversity (e.g. Dwyer *et al.* 1999). The radiant energy released per unit time during a vegetation fire is directly related to the amount of biomass burning and combustion gases emitted to the atmosphere (Wooster *et al.* 2005). As wild fires are generally associated with vegetation combustion at temperatures within the 600–1300 K range, they exhibit an emission peak in the mid-IR (3–5 μm), in accordance with Wien's displacement law. Therefore, the detection of active fires is essentially based on the signature of these events (even with subpixel scales) on the brightness temperature of channel IR3.9. The algorithm used by the Land-SAF for fire detection is based on a series of contextual thresholds, derived empirically for channels IR3.9 and IR10.8, which take into account values of immediate (fire-free) neighbours (Giglio *et al.* 2003). The Land-SAF currently produces Fire Radiative Power (FRP) at the pixel scale (every 15-min; figure 9), and at a coarser resolution (1° longitude × 1° latitude; hourly), following the algorithm described in Wooster *et al.* (2005). The rate of radiant energy emitted by a fire (FRP) is estimated using the Planck function, relating the emitted spectral radiance and the emitter temperature (Wooster *et al.* 2003).

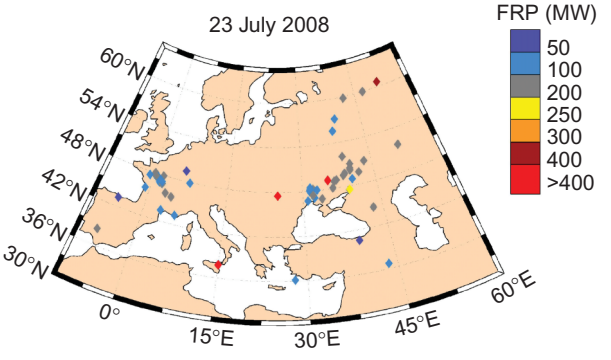

Figure 9. Fire Radiative Power (FRP) corresponding to all fire events detected over Europe on 23 July 2008. The point over Sicily corresponds to the volcano in Mount Etna.

Validation of the detection of wild-fire events and corresponding radiative power obtained from SEVIRI/MSG is mostly based on comparisons with similar MODIS products. The higher spatial resolution of the MODIS instrument allows the identification of significantly more events (weak or small fires) than SEVIRI; for simultaneous observations SEVIRI misses up to 50–55% of fires detected by MODIS. In addition, the higher dynamic range of MODIS allows the estimation of higher FRP values than SEVIRI, which saturates at lower temperatures. However, because of its high (15-min) sampling rate, SEVIRI is likely to capture a signal from most fire events, in contrast to MODIS, with only four overpasses per day. SEVIRI is able to observe a significant part of the life-cycle of wild fires, and thus capture most events when they reach their peak intensity. Moreover, the FRP estimations using SEVIRI will be far more representative of the radiative energy released over a day by wild fires than those provided by instruments on polar orbiters, such as MODIS (Govaerts *et al.* 2008).

4. Conclusion

After a 5-year development phase and a 2-year period in pre-operation, the Land-SAF Team has a set of consolidated algorithms, used to generate land surface products in an operational mode, which are archived and disseminated in near real time or off-line. These include retrievals of surface radiative components, vegetation parameters and snow cover. Other algorithms are already in an advanced stage of development and foreseen to become operational during the current 5-year phase of the project (2007–2012). All of the products are distributed with quality control information and for some of them with an error range, indicative of the expected accuracy of the retrieved fields, on a pixel-by-pixel basis, supported by sensitivity studies and product validation.

Product validation is an essential component of Land-SAF activities, as the main source of information on the compliance of generated products with user requirements. Only parameters that meet the target accuracy described in table 2 for a significant number of cases are considered operational (i.e. are distributed to users). Furthermore, the results of product validation are one of the drivers for further algorithm development and improvements of the quality of products. Validation activities basically consist of intercomparison of Land-SAF products and similar parameters retrieved from other satellite data (e.g. LST retrieved from AATSR on ENVISAT, LST and AL from MODIS on EOS, vegetation parameters from MERIS on ENVISAT, MODIS on EOS, snow cover from NOAA/NESDIS and MODIS) and with ground-truth sites. Such intercomparison exercises are often carried out in cooperation with existing projects or networks of detailed *in situ* measurements (e.g. BSRN, GEWEX). Given the lack of LST ground measurements within the Meteosat disc, the Land-SAF Team has set up its own sites, which are particularly dedicated to LST, but that also collect downward surface radiative fluxes and other meteorological data. The first of these stations has been set up in Évora (Southern Portugal), while two others have recently been installed in Namibia and Senegal.

The Land-SAF addresses a wide community, ranging from surface processes modelling (e.g. NWP, seasonal forecasting and climate models) to agriculture and forestry applications (e.g. fire hazards, food production) and hydrology. This community greatly benefits from products generated from a reliable observation system designed to ensure long-term operations. The MSG programme alone is expected to provide observations for at least 12 years (e.g. Schmetz *et al.* 2002), while Meteosat

Third Generation is already under preparation. Both Meteosat and MetOp series are important components of the Global Earth Observation System of Systems (GEOSS), a comprehensive, sustained observation system of the Earth. It is the role of the Land-SAF, and all SAFs in general, to adapt existing algorithms to forthcoming (EUMETSAT) sensors, guaranteeing the continuation of current products, and to develop applications that fully exploit new remote sensing capabilities.

The Land-SAF products, classified as 'essential' by EUMETSAT, are available on a free and unrestricted basis. The data may be requested and downloaded off-line from the Land-SAF website, while near-real-time users are encouraged to use EUMETCast, which is the primary distribution means for EUMETSAT image data and derived products. Additional information on the Land-SAF is available at http://landsaf.meteo.pt/, while the EUMETSAT website at www.eumetsat.int provides details on European meteorological satellites and other SAFs.

Acknowledgements

The Land-SAF project is funded by EUMETSAT. The authors would like to express their gratitude to various people involved in the project team, whose efforts have been essential for the success of the Land-SAF. *In situ* data are essential for validation purposes; most data used for the validation of radiation fluxes were obtained from BSRN stations; observations of evapotranspiration in Cabauw were kindly provided by F. Bosveld.

References

Allan, R.P., Ringer, M.A., Pamment, J.A. and Slingo, A., 2004, Simulation of the Earth's radiation budget by the European Centre for Medium-Range Weather Forecasts 40-year reanalysis (ERA40). *Journal of Geophysical Research*, **109**, D18107, doi:10.1029/2004JD004816

Barroso, C, Trigo, I.F., Olesen, F., DaCamara, C. and Queluz, M.P., 2005, Intercalibration of NOAA and Meteosat window channel brightness temperatures. *International Journal of Remote Sensing*, **26**, pp. 3717–3733.

Bateson, C.A., Asner, G.P. and Wessman, C.A., 2000, Endmember bundles: a new approach to incorporating endmember variability into spectral mixture analysis. *IEEE Transactions on Geosciences and Remote Sensing*, **38**, pp. 1083–1094.

Beljaars, A.C.M. and Bosveld, F.C., 1997, Cabauw data for the validation of land surface parameterization schemes. *Journal of Climate*, **10**, pp. 1172–1193

Boschetti, L., Brivio, P.A. and Gregoire, J.M., 2003, The use of Meteosat and GMS imagery to detect burned areas in tropical environments. *Remote Sensing of Environment*, **81**, pp. 78–91.

Brisson, A., Le Borgne, P. and Marsouin, A., 1999, *Development of Algorithms for Surface Solar Irradiance Retrieval at O&SI SAF Low and Mid Latitudes* (Lannion: Météo-France/CMS).

Bony, S., Colman, R., Kattsov, V.M., Allan, R.P., Bretherton, C.S., Dufresne, J.-L., Hall, A., Hallegatte, S., Holland, M.M., Ingram, W., Randall, D.A., Soden, B.J., Tselioudis, G. and Webb, M.J., 2006, How well do we understand and evaluate climate change feedback processes? *Journal of Climate*, **19**, pp. 3445–3482.

Caparrini, F., Castelli, F. and Entekhabi, D., 2004, Estimation of surface moisture control and turbulent transfer by assimilating sequences of radiometric surface temperature measurements. *Journal of Hydrometeorology*, **5**, pp. 145–159.

Clerbaux, N., Bertrand, C., Caprion, D., Depaepe, B., Dewitte, S., Gonzalez, L. and Ipe, A., 2005, Narrowband-to-broadband conversions for SEVIRI. In *Proceedings of the 2005 EUMETSAT Meteorological Satellite Conference*, Dubrovnik, pp. 351–357, Available

online at: http://www.eumetsat.int/Home/Main/AboutEUMETSAT/Publications/index.htm.

Crutzen, P. and Andreae, M.O., 1990, Biomass burning in the tropics: impact on atmospheric chemistry and biogeochemical cycles. *Science*, **250**, pp. 1669–1678.

Dickinson, R.E., 1983, Land surface processes and climate – surface albedos and energy balance. *Advances in Geophysics*, **25**, pp. 305–353.

Dirmeyer, P.A., Gao, X., Zhao, M., Guo, Z., Oki, T. and Hanasaki, N., 2006, GSWP-2: multimodel analysis and implications for our perception of the land surface. *Bulletin of the American Meteorological Society*, **87**, pp. 1381–1397.

Drusch, M., Vasiljevic, D. and Viterbo, P., 2004, ECMWF's global snow analysis: assessment and revision based on satellite observations. *Journal of Applied Meteorology*, **45**, pp. 1282–1294.

Dwyer, E., Pereira, J.M.C., Gregoire, J.P. and DaCamara, C.C, 1999, Characterization of the spatio-temporal patterns of global fire activity using satellite imagery for the period April 1992 to March 1993. *Journal of Biogeography*, **27**, pp. 57–69.

Freitas, S., Trigo, I.F., Bioucas-Dias, J. and Göttsche, F., 2010, Quantifying the uncertainty of land surface temperature retrievals from SEVIRI/Meteosat. *IEEE Transactions on Geoscience and Remote Sensing*, **48**, pp. 523–534.

Frouin, R., Lingner, D.W., Gautier, C., Baker, K.S. and Smith, R.C., 1989, A simple analytical formula to compute clear sky total and photosynthetically available solar irradiance at the ocean surface. *Journal of Geophysical Research*, **94**, pp. 9731–9742.

García-Haro, F.J., Sommer, S. and Kemper, T., 2005, Variable multiple endmember spectral mixture analysis (VMESMA). *International Journal of Remote Sensing*, **26**, pp. 2135–2162.

Gautier, C., Diak, G. and Masse, S., 1980, A simple physical model to estimate incident solar radiation at the surface from GOES satellite data. *Journal of Climate and Applied Meteorology*, **19**, pp. 1005–1012.

Geiger, B., Carrer, D., Franchistéguy, L., Roujean, J.-L. and Meurey, C., 2008a, Land surface albedo derived on a daily basis from Meteosat second generation observations. *IEEE Transactions on Geoscience and Remote Sensing*, **46**, pp. 3841–3856.

Geiger, B., Meurey, C., Lajas, D., Franchistéguy, L., Carrer, D. and Roujean, J.-L., 2008b, Near real-time provision of downwelling shortwave radiation estimates derived from satellite observations. *Meteorological Applications*, **15**, pp. 411–420.

Giglio, L., Descloitres, J., Justice, C.O. and Kaufman, Y.J., 2003, An enhanced contextural fire detection algorithm for MODIS. *Remote Sensing of Environment*, **87**, pp. 273–282.

Govaerts, Y., Wooster, M., Lattanzio, A., Roberts, G., Freeborn, P., Xu, W. and Trigo, I., 2008, The operational MSG/SEVIRI fire radiative power product generated at the Land SAF. In *Proceedings of the 2008 EUMETSAT Meteorological Satellite Conference*, Darmstadt. Available online at: www.eumetsat.int/Home/Main/AboutEUMETSAT/Publications/.

Harries, J.E., Russell, J.E., Hanafin, J.A., Brindley, H., Futyan, J., Rufus, J., Kellock, S., Matthews, G., Wrigley, R., Last, A., Mueller, J., Mossavati, R., Ashmall, J., Sawyer, E., Parker, D., Caldwell, M., Allan, P.M., Smith, A., Bates, M.J., Coan, B., Stewart, B.C., Lepine, D.R., Cornwall, L.A., Corney, D.R., Ricketts, M.J., Drummond, D., Smart, D., Cutler, R., Dewitte, S., Clerbaux, N., Gonzalez, L., Ipe, A., Bertrand, C., Joukoff, A., Crommelynck, D., Nelms, N., Llewllyn-Jones, D.T., Butcher, G., Smith, G.L., Szewczyk, Z.P., Mlynczak, P.E., Slingo, A., Allan, R.P. and Ringer, M.A., 2005, The Geostationary Earth Radiation Budget Project. *Bulletin of the American Meteorological Society*, **86**, pp. 945–960.

Huemmrich, K.F., Privette, J.L., Mukelabai, M., Myneni, R.B. and Knyazikhin, Y., 2005, Time-series validation of MODIS land biophysical products in a Kalahari woodland, Africa. *International Journal of Remote Sensing*, **26**, pp. pp. 4381–4398.

Josey, S.A., Pascal, R.W., Taylor, P.K. and Yelland, M.J., 2003, A new formula for determining the atmospheric longwave flux at the ocean surface at mid-high latitudes. *Journal of Geophysical Research*, **108**, 3108, doi:10.1029/2002JC001418.

KABSCH, E., OLESEN, F.S. and PRATA, 2008, Initial results of the land surface temperature (LST) validation with the Evora, Portugal ground-truth station measurements. *International Journal of Remote Sensing*, **29**, pp. 5329–5345.

KONGOLI, C., GRODY, N.C. and FERRARO, R.R., 2004, Interpretation of AMSU microwave measurements for the retrievals of snow water equivalent and snow depth. *Journal of Geophysical Research*, **109**, D24111, doi:10.1029/2004JD004836.

LAND-SAF, 2006, *Product User Manual: Snow Cover.* SAF/LAND/FMI/PUM/SC/2.5. Available online at: http://landsaf.meteo.pt.

LAND-SAF, 2008, *Validation Report: Evapotranspiration.* SAF/LAND/RMIB/VR_MET_0.3. Available online at: http://landsaf.meteo.pt.

MANALO-SMITH, N., SMITH, G.L., TIWARI, S.N. and STAYLOR, W.F., 1998, Analytic forms of bi-directional reflectance functions for application to Earth radiation budget studies. *Journal of Geophysical Research*, **103D**, pp. 19733–19751.

NORMAN, J.M. and BECKER, F., 1995, Terminology in thermal infrared remote sensing of natural surfaces. *Agricultural and Forest Meteorology*, **77**, pp. 153–166.

OHMURA, A., DUTTON, E.G., FORGAN, B., FRÖHLICH, C., GILGEN, H., HEGNER, H., HEIMO, A., KÖNIG-LANGLO, G., MCARTHUR, B., MÜLLER, G., PHILIPONA, R., PINKER, R., WHITLOCK, C.H., DEHNE, K. and WILD, M., 1998, Baseline Surface Radiation Network (BSRN/WRMC), a new precision radiometry for climate research. *Bulletin of the American Meteorological Society*, **79**, pp. 2115–2136.

PEREIRA, J.M.C. and GOVAERTS, Y., 2001, *Potential Fire Applications from MSG/SEVIRI Observations.* EUMETSAT Programme Development Department, Technical Memorandum No. 7.

PERES, L.F. and DACAMARA, C.C., 2005, Emissivity maps to retrieve land-surface temperature from MSG/SEVIRI. *IEEE Transactions on Geosciences and Remote Sensing*, **43**, pp. 1834–1844.

PRATA, A.J., 1996, A new long-wave formula for estimating downward clear-sky radiation at the surface. *Quarterly Journal of the Royal Meteorological Society*, **122**, pp. 1121–1151.

PRIVETTE, J.L., MYNENI, R.B., KNYAZIKHIN, Y., MUKELABAI, M., ROBERTS, G., TIAN, Y., WANG, Y. and LEBLANC, S.G., 2002, Early spatial and temporal validation of MODIS LAI product in the Southern Africa Kalahari. *Remote Sensing of Environment*, **83**, pp. 232–243.

RAHMAN, H. and DEDIEU, G., 1994, SMAC: a simplified method for the atmospheric correction of satellite measurements in the solar spectrum. *International Journal of Remote Sensing*, **15**, pp. 123–143.

ROUJEAN, J.-L. and BRÉON, F.M., 1995, Estimating PAR absorbed by vegetation from bidirectional reflectance measurements. *Remote Sensing of Environment*, **51**, pp. 375–384.

ROUJEAN, J.-L. and LACAZE, R., 2002, Global mapping of vegetation parameters from POLDER multiangular measurements for studies of surface-atmosphere interactions: a pragmatic method and its validation. *Journal of Geophysical Research*, **107D**, pp. 1–14.

ROUJEAN, J.-L., LEROY, M. and DESCHAMPS, P.-Y., 1992, A bidirectional reflectance model of the Earth's surface for the correction of remote sensing data. *Journal of Geophysical Research*, **97D**, pp. 20455–20468.

SCHMETZ, J., PILI, P., TJEMKES, S., JUST, D., KERKMAN, J., ROTA, S. and RATIER, A., 2002, An introduction to Meteosat Second Generation (MSG). *Bulletin of the American Meteorological Society*, **83**, pp. 977–992.

SLINGO, A., ACKERMAN, T.P., ALLAN, R.P., KASSIANOV, E.I., MCFARLANE, S.A., ROBINSON, G.J., BARNARD, J.C., MILLER, M.A., HARRIES, J.E., RUSSELL, J.E. and DEWITTE, S., 2006, Observations of the impact of a major Saharan dust storm on the atmospheric radiation balance. *Geophysical Research Letters*, **33**, L24817, doi:10.1029/2006GL027869.

TRIGO, I.F., MONTEIRO, I.T., OLESEN, F. and KABSCH, E., 2008a, An assessment of remotely sensed land surface temperature. *Journal of Geophysical Research*, **113**, D17108, doi:10.1029/2008JD010035.

Trigo I.F., Peres, L.F., DaCamara, C.C. and Freitas, S.C., 2008b, Thermal land surface emissivity retrieved from SEVIRI/Meteosat. *IEEE Transactions on Geosciences and Remote Sensing*, **46**, pp. 307–3157.

Wan, Z. and Dozier, J., 1996, A generalized split-window algorithm for retrieving land surface temperature from space. *IEEE Transactions on Geosciences and Remote Sensing*, **34**, pp. 892–905.

Wooster, M.J., Roberts, G., Perry, G. and Kaufman, Y.J., 2005, Retrieval of biomass combustion rates and totals from fire radiative power observations: calibration relationships between biomass consumption and fire radiative energy release. *Journal of Geophysical Research*, **110**, D21111, doi:10.1029/2005JD006318.

Wooster, M.J., Zhukov, B. and Oertel, D., 2003, Fire radiative energy for quantitative study of biomass burning from the BIRD experimental satellite and comparison to MODIS fire products. *Remote Sensing of Environment*, **86**, pp. 83–107.